Supporting Information

Single-Molecule Detection of Airborne Singlet Oxygen

Kazuya Naito, Takashi Tachikawa, ShiCong Cui, Akira Sugimoto, Mamoru Fujitsuka,

and Tetsuro Majima*

The Institute of Scientific and Industrial Research (SANKEN), Osaka University, Mihogaoka 8-1, Ibaraki, Osaka 567-0047, Japan

Contents

S1. Short Historical Review of $^1O_2$ Detection and Photocatalytic Reaction Schemes

The $^1O_2$ molecule is known to be a highly energetic oxygen molecule, which can oxidize organic molecules, resulting in the photodegradation. In the early 1930s, Kautsky suggested the possibility that $^1O_2$ molecules might be involved as the reactive intermediate during dye-sensitized photooxygenation reactions.[1] He demonstrated that excitation of sensitizer molecules adsorbed on silica gel caused the oxygenation of acceptor molecules absorbed on a different set of silica gel particles, which are physically separated from the dye-coated ones.[1d] From this experimental result, it was concluded that the oxygenation must have involved formation of some metastable species which was capable of migrating in the gas phase from the sensitizer to the acceptor, and suggested that this species was $^1O_2$ molecules. Although Kautsky's proposal was not generally accepted during his lifetime, it was eventually supported by later works by the groups of Khan and Kasha,[2] Foote and Wexler,[3] and Corey and Taylor.[4] To date, variants of the Kautsky experiment have been performed,[5,6] and the development of both applications and novel observation techniques has strongly accelerated in the past decade.[7] In the present work, we report a modern version of the Kautsky experiment using TiO_2 photocatalyst as a sensitizer.

It is well-known that electron-hole pairs are generated when TiO_2 is irradiated by UV photons with an energy higher than the TiO_2 band gap energy, and these charge carriers can then migrate to the TiO_2 surface to initiate various redox reactions of the adsorbates. Such interfacial electron (hole) transfer reactions are fundamental processes in water-splitting reaction for hydrogen evolution, the degradation of organic pollutants, the surface wettability conversion, and so on.[8]

Recently, it has been reported that $^1O_2$ molecules are generated during the TiO_2 photocatalytic reactions.[9,10] Nosaka et al. reported the direct observation of the formation of $^1O_2$ in a TiO_2 aqueous suspension and roughly estimated the quantum yield of $^1O_2$ (about 0.2) by comparing with that (0.84) for Rose Bengal and by accounting for the incident intensities of laser light and the absorbance at the excitation wavelength.[9] On the other hand, Hirakawa and Hirano reported the quantum yield of about 0.02 for both types of TiO_2 photocatalysts, i.e., anatase and rutile, in ethanol by comparing with that

(0.52) for Methylene Blue and by accounting for the lifetimes of $^1O_2$ (5 and 12 µs for TiO_2 and Methylene Blue, respectively).[10]

The formation mechanisms of $^1O_2$ can be described as the photocatalytic oxidation of superoxide ($O_2^{\bullet-}$) back to $^1O_2$ molecules as follows: reaction (1), the conduction electron, e^-, and the valence hole, h^+, are generated after UV irradiation of TiO_2, reaction (2), $O_2^{\bullet-}$ is produced by the reduction of $^3O_2$ molecules with e^-, and reaction (3), $O_2^{\bullet-}$ is oxidized back to $^1O_2$ molecule by h^+, resulting in $^1O_2$ on the TiO_2 surface.[9]

$$TiO_2 + hv \rightarrow e^- + h^+, \tag{1}$$

$$^3O_2 + e^- \rightarrow O_2^{\bullet-}, \tag{2}$$

$$O_2^{\bullet-} + h^+ \rightarrow \ ^1O_2 \text{ and } ^3O_2, \tag{3}$$

Otherwise, $^1O_2$ is also generated by the energy exchange between the excited TiO_2 and $^3O_2$ molecules.[11]

$$TiO_2 + \ hv \rightarrow TiO_2^{*}, \tag{4}$$

$$TiO_2^{*} + \ ^3O_2 \rightarrow TiO_2 + \ ^1O_2, \tag{5}$$
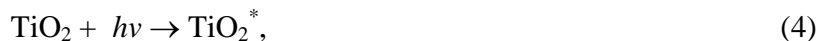
However, this is considered not to be dominant when compared to that of the photocatalytic oxidation of $O_2^{\bullet-}$. In the remote TiO_2 photocatalytic oxidation, $^1O_2$ generated on the TiO_2 surface is considered to barely diffuse into the gas phase forming airborne $^1O_2$.

In the present system, we can not claim that $^1O_2$ is sole reactive species. Other reactive species, such as $^{\bullet}OH$ and H_2O_2, would be generated during the TiO_2 photocatalytic reactions. For example, $^{\bullet}OH$ is generated as described by reaction (6),[8]

$$h^+ + H_2O \text{ (or OH}^-) \rightarrow \ ^{\bullet}OH + H^+ \text{ (or } ^{\bullet}OH), \tag{6}$$
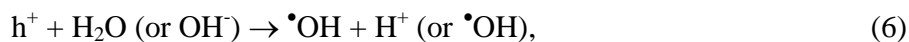
H_2O_2 can also be generated from $^{\bullet}OH$ as follows,

$$2^{\bullet}OH \rightarrow H_2O_2. \tag{7}$$

To date, the remote TiO_2 photocatalytic oxidation has been successfully applied to various organic and inorganic substrates such as the saturated alkyl chain monolayer, polymer, carbon soot, copper, and

silicon carbide,[12-15] suggesting that only •OH is capable enough to oxidize such diverse materials. More recently, Nosaka et al. successfully detected •OH diffused in the gas phase from the photocatalytic TiO$_2$ surfaces using the in situ laser-induced fluorescence technique.[16]

According to the literatures and the present results, it is strongly believed that both $^1O_2$ and •OH (or H$_2$O$_2$) are generated during the TiO$_2$ photocatalytic reactions, and diffused into the gas phase. As reported elsewhere,[17] the fact that a relatively low bleaching rate of single dye molecules (Alexa Fluor 532, Molecular Probes) immobilized onto a glass coverslip was observed for the H$_2$O$_2$-coated glass, compared with the TiO$_2$-coated glass, suggest that •OH is *not* sole reactive species.

S2. Experimental and Analytical Procedures

Sample preparation. TDI was synthesized according to the procedures reported by Müllen et al.[18] The absorption and emission spectra of TDI are shown in Figure S1. The peak wavelengths of the absorption and emission are 655 and 670 nm, respectively.
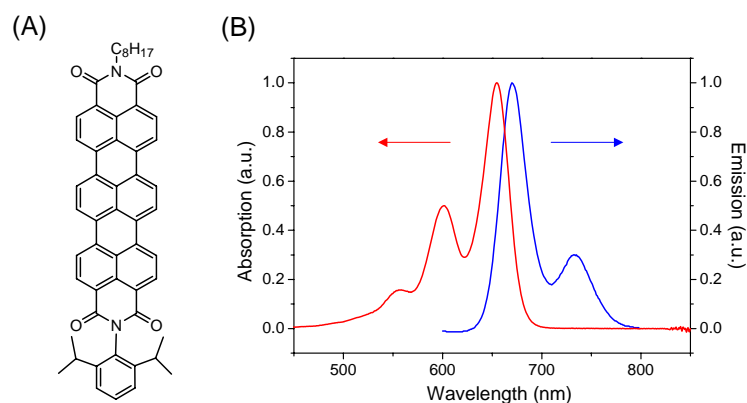
Figure S1. (A) Molecular structure of TDI and (B) solution absorption (red) and emission (blue) spectra of TDI measured in CHCl$_3$ solution. The emission spectrum was obtained from excitation at 532 nm. The steady-state UV-Vis absorption and fluorescence spectra were measured using a Shimadzu UV-3100 and a Hitachi 850, respectively.

CHCl$_3$ and toluene were purchased from Wako, and poly(methylmethacrylate) (PMMA) (M_w = 15 000) was purchased from Aldrich. All the reagents were used as supplied.

The cover glasses were purchased from Matsunami Glass and cleaned by sonication in a 20% detergent solution (As One, Cleanace) for 6 h, followed by repeated washing with warm running water for 30 min. Finally, the cover glass was washed again with Milli-Q water.

Samples for the single-molecule experiments were prepared by first spin-coating a toluene solution of PMMA (40 μl, 10 gl^{-1}) on a clean cover glass at 3000 rpm for 15 s, followed by spin-coating a chloroform solution of TDI (40 μl, 3 nM) at 3000 rpm for 15 s. The sequence of the spin-coating in preparing the samples is very important. The PMMA film should be spin-coated prior to the TDI. In the control experiment, the samples were prepared by spin-coating TDI, followed by spin-coating PMMA. This sample is called the "top-coat".

Although PMMA cannot extensively react with $^1O_2$,[19] PMMA can react with the radical oxygen species generated during the TiO_2 photocatalytic reaction, such as the hydroxyl radical ($^\bullet OH$) or hydroperoxyl radical ($^\bullet HO_2$).[20] Thus, the underlaying PMMA film allows TDI to selectively react with $^1O_2$ diffusing through the gas phase from the TiO_2 surface, and the contribution of the radicals in the decomposition of TDI is excluded. PMMA also protects TDI from excess $^3O_2$, which causes TDI to be oxidized due to $^1O_2$ formed by a self-sensitization process through the interaction with an electronically excited TDI.[21]

Quenching of $^1O_2$ by TDI in bulk solution. To examine the bimolecular reaction between $^1O_2$ and TDI, we measured the decay kinetics of $^1O_2$ phosphorescence, which has a band maximum centered at about 1270 nm, in air-saturated toluene-d_8 (Nacalai Tesque, 99.6 atom % D) at room temperature. The lifetime of $^1O_2$ is reported to be 0.31 ± 0.02 ms in air-saturated toluene-d_8.[22] Here, we used C_{60} (Tokyo Kasei, >99.5%) as a sensitizer to produce $^1O_2$ (the quantum yield for $^1O_2$ formation is 0.76 ± 0.05 in benzene).[23] No electronic interaction between C_{60} and TDI in the ground state was confirmed by steady-state UV-Vis absorption measurements. $^1O_2$ phosphorescence decay curves were measured as summarized in the followings. A third harmonic generation (355 nm, 5 ns fwhm) from a Q-switched Nd^{3+}:YAG laser (Continuum, Surelite II-10) was used as the excitation source to generate C_{60} in the triplet excited state ($^3C_{60}{}^*$). The unfocussed laser beam was attenuated by being passed through an

aperture and a bandpass filter (centered at 350 nm, fwhm = ca. 50 nm), and the total energy incident at the cuvette was ca. 1 mJ pulse^{-1}. A sample cell was held in a specially designed holder placed just ahead of a lens adapter, which was used to focus the signal light onto the detector. A cutoff filter (< 1000 nm) was placed between the lens adapter and the sample holder to cut off unwanted scattered laser light. The phosphorescence of $^1O_2$ was detected by a photomultiplier tube (Hamamatsu Photonics, R5509-72), which was located in the chamber (Hamamatsu Photonics, C6544-20) cooled at -80 °C utilizing liquid nitrogen as the coolant medium. The transient signals were recorded with a digitizer (Tektronix, TDS 580D). The reported signals are averages of 100 events.

Figure S2 shows the TDI concentration dependence of the decay kinetics of $^1O_2$ phosphorescence observed during the 355-nm laser photolysis of C_{60} ([C_{60}] = 25 μM) in air-saturated toluene-d_8 at room temperature. The decay rates were determined by the single-exponential fitting of the kinetic traces to the expression for a quasi-first-order reaction. From the relationship between the observed quenching rates (k_q^{obs}) and TDI concentrations, the bimolecular quenching rate constant (k_q) was determined to be $(2.6 \pm 0.2) \times 10^9$ M^{-1} s^{-1}. This value suggests that $^1O_2$ molecules are quenched by TDI with nearly diffusion-controlled kinetics (ca. $10^9 \sim 10^{10}$ M^{-1} s^{-1} at room temperature).
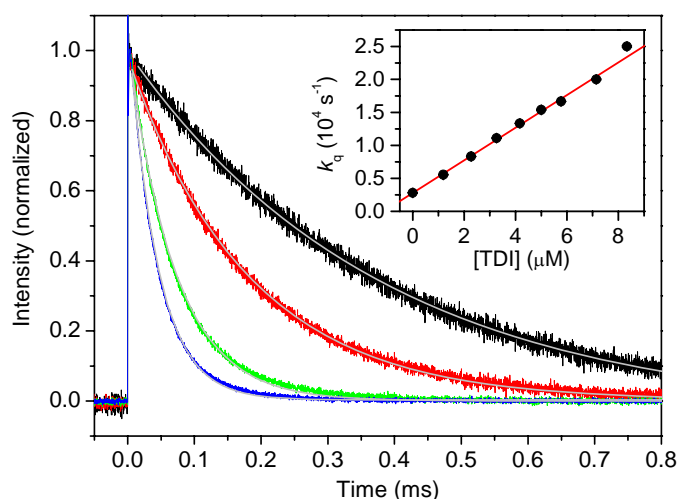
Figure S2. Kinetic traces of $^1O_2$ phosphorescence, which has a band maximum centered at about 1270 nm, observed during the 355-nm laser photolysis of C_{60} ([C_{60}] = 25 μM) in air-saturated toluene-d_8. The concentrations of TDI are 0 (black), 1.2 (red), 5.0 (green), and 8.3 μM (blue). The gray lines represent nonlinear least squares curve fits. Inset shows the relationship between the observed quenching rates (k_q^{obs}) and TDI concentrations. The bimolecular quenching reaction rate constant (k_q) was determined to be $(2.6 \pm 0.2) \times 10^9$ M^{-1} s^{-1}.

Estimation of the thickness of PMMA film. To estimate the thickness of the PMMA film, we measured the SEM images of the PMMA-coated coverslip (FE-SEM, JEOL, JSM-6330FT). The SEM images are shown in Figure S3. The thickness of the PMMA film is estimated to be approximately 14 nm. This value is smaller than the penetration depth of the evanescent field (approximately 100 nm from coverslip-air interface). It is suggested that TDI molecules on the PMMA-coated coverslip can be excited by the evanescent field.


200 μm   **200 nm**
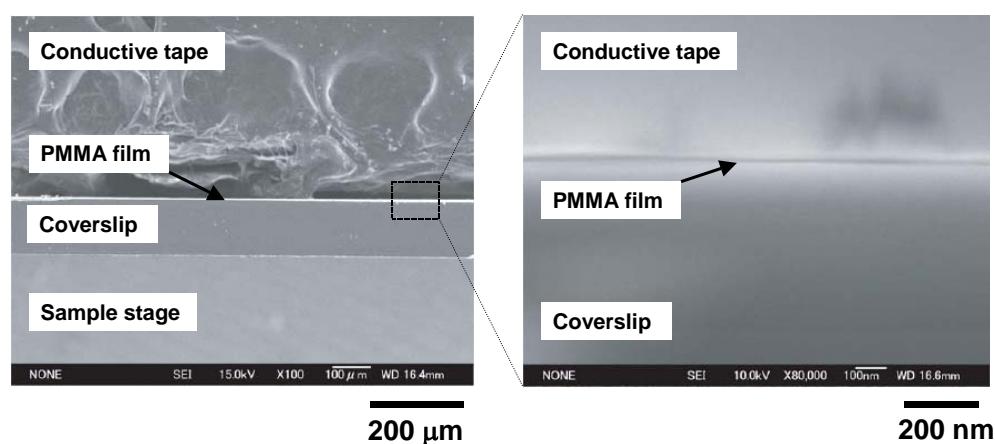
Figure S3. SEM images of a PMMA-coated coverslip. The thickness of the PMMA film is estimated to be approximately 14 nm.

Preparation of the TiO₂ film. A TiO$_2$ aqueous sol STS-21 (Ishihara Sangyo) was diluted with Milli-Q water (80 vol%), sonicated overnight, and coated on a slide glass (Matsunami Glass) by spin coating at 2000 rpm for 15 s. The resulting TiO$_2$ film was calcined at 400 °C for 1 h to obtain an optically opaque TiO$_2$ coated glass plate. The resulting TiO$_2$ film was irradiated by a UV lamp overnight before the experiment to clean the surface. The film thickness was determined to be 1 μm using a Veeco Instruments Dektak3 surface profiler. The value of the absorbance at 365 nm is about 0.3. The TiO$_2$ film was irradiated with a 100-W mercury lamp (0.2 mW cm^{-2}) (Ushio, USH-102D) through a 365 nm band-pass filter (Olympus, U-MWU2). The irradiation energy was directly measured using a power meter (Ophir, OrionTH). The gap between the TiO$_2$ film and the TDI-coated glass was controlled using polyimide films (Nilaco, thickness, 12.5-2000 μm). As reported elsewhere, the remote oxidation rate strongly depends on the oxygen concentration, but poorly on the humidity.[10] For the control experiment

under an argon atmosphere, the TiO$_2$-coated slide glass is drilled to make air holes around the observation region in order to efficiently purge the argon atmosphere.

Detection system of airborne ^{1}O$_2$. Schematic illustration of the experimental setup is shown in Figure S4. The sample is composed of the TiO$_2$ film-coated slide glass and TDI-coated cover glass with an intervening gap. The TiO$_2$ film is irradiated with UV light (365 nm, 0.2 mW cm^{-2}, Ushio, USH-102D) to generate ^{1}O$_2$ on the TiO$_2$ surface. To observe the reaction between TDI and ^{1}O$_2$, TDI on the cover glass is observed with an evanescent field generated by a continuous wave (CW) Nd:YAG laser (532 nm, 50 mW; JDS Uniphase, 4611-050) totally reflected at the cover glass-air interface. Air holes are made on the TiO$_2$-coated slide glass to efficiently purge the gas into the sample.
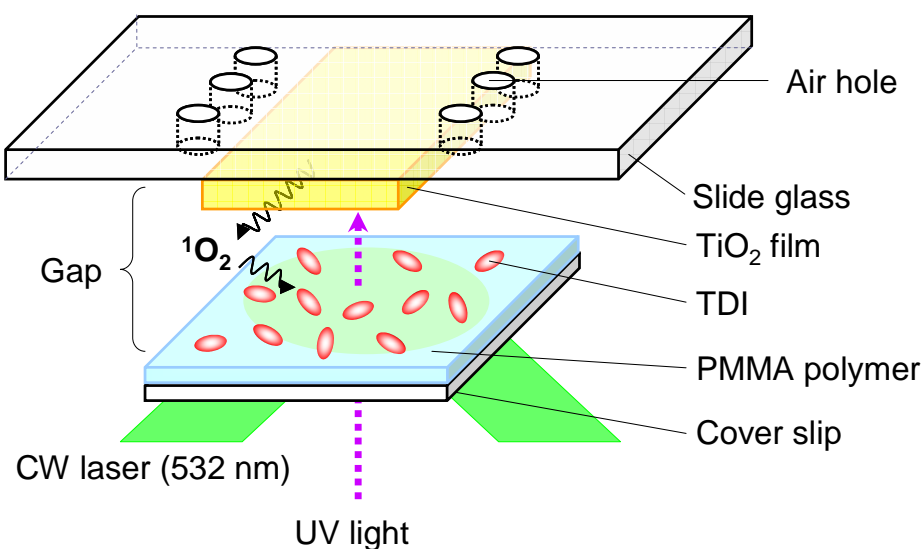
Figure S4. Schematic representation of the experimental setup. The TiO$_2$ film is irradiated with UV light (365 nm), and then ^{1}O$_2$ is generated on the TiO$_2$ surface. ^{1}O$_2$ is desorbed from the surface, and diffused in the gas phase (airborne ^{1}O$_2$). Airborne ^{1}O$_2$ added to the TDI on the coverslip to form the endoperoxide, accompanied by the spectral blue-shift. This reaction is observed by an evanescent field, which is generated from the CW laser (532 nm) totally reflected at the cover glass-air interface.

Single-molecule fluorescence measurements. The experimental setup is based on an Olympus IX71 inverted fluorescence microscope. Light emitted from a continuous wave Nd:YAG laser (532 nm, 50 mW; JDS Uniphase, 4611-050) passing through an objective lens (Olympus, PlanApo, 1.45 NA, 100×) was totally reflected at the cover glass-air interface to obtain an evanescent field which can excite a dye

molecule. All the experimental data were obtained at room temperature. The atmosphere in the experiment is controlled as ambient air or argon as appropriate.

For imaging, the fluorescence emission from single dyes was collected using an oil-immersion microscope objective and intensified by an image intensifier (Hamamatsu Photonics, C8600-03) coupled to a CCD camera (Hamamatsu Photonics, C3077-70). The images were recorded on a video cassette recorder at the video frame rate of 30 frames s^{-1}. The pictures recorded on the videotape were converted into an electronic movie file using the ADVC 1394 video capture board (Canopus).

For spectroscopy, only the fluorescence that passed through a slit entered the imaging spectrograph (Acton Research, SP-2356) equipped with an electron-multiplying charge coupled device (EMCCD) camera (Princeton Instruments, PhotonMAX:512B). The width of the slit was 200 μm, which corresponded to 1.25 μm at the specimen, because the images at the slit were magnified by 160×. The spectra were typically integrated for 10 s. The fluorescence spectra were cut by a dichroic mirror (Olympus, DM570) and a long-pass filter (Olympus, BA575IF) on the blue edge. The spectrum detected by the EMCCD camera was stored and analyzed using a personal computer.

The acquisition procedures of the single-molecule spectrum are described in Figure S5. The fluorescence spectra through a slit are imaged as a diffraction pattern. Each horizontal stripe in the diffraction pattern (Figure S5C, as shown in red) corresponds to the fluorescence of a single TDI molecule. The diffraction pattern enables us to distinguish the spectral shift toward shorter wavelengths at the single-molecule level. An example of "digital switching", that is, the blue shift of a single-molecule fluorescence spectrum, is shown in Figure S6. The fluorescence spectra of single TDI molecules indicate the digital switching by the reaction with $^1O_2$ (Figure S6A and B). To clarify whether or not the digital switching occurs at the same position, the cross sections of the diffraction pattern before and after UV irradiation were obtained, as shown in Figure S6C. The TDI molecules that show the digital switching are indicated (see arrows in Figure S6C). Some TDI molecules (for example, at 260 pixels) disappear after UV irradiation. This would arise from the irreversible photobleaching. In contrast, after UV irradiation, two molecules (approximately 150 pixels) appear in which there is no

molecule before the UV irradiation. This should be due to the addition of $^1O_2$ to TDI, which is in the dark state, such as the triplet state, before UV irradiation. Under this experimental condition, 40% of the TDI molecules show complete digital switching.

Figure S5. Schematic representation of the acquisition of the fluorescence spectra of single TDI molecules.

Figure S6. The digital switching toward shorter wavelength arising from the oxidation of TDI during UV irradiation. The diffraction pattern of the single-molecule spectra before (A) and after (B) UV irradiation for 5 min. The cross section of the diffraction pattern before (C, black) and after (C, red) UV irradiation. The positions of the cross section before and after UV irradiation are indicated as dotted lines in (A) and (B), respectively. The molecules that show the digital switching are indicated (arrows).

Estimation of the generation efficiency of airborne $^1O_2$. We investigated the generation efficiency of airborne $^1O_2$ based the spatial and temporal distributions of the $^1O_2$ molecules. When the reaction yield of the cycloaddition is assumed to be 1.0, the generation efficiency is defined as the ratio of the number of photons absorbed by TiO_2 (N_{ph}) and the number of airborne $^1O_2$ near the surface of the TiO_2 nanoparticle (N_0), which is estimated by extrapolating the intervening gap to zero, as described by the following equation,

$$\text{The generation efficiency of airborne } ^1O_2 = \frac{\text{The number of airborne } ^1O_2 \text{ near the } TiO_2 \text{ surface } (N_0)}{\text{The number of photon absorbed by } TiO_2 (N_{ph})}.$$

N_{ph} can be estimated by considering the power of the UV lamp (0.2 mW cm^{-2}), the area of the UV-irradiated region (diameter 10 μm), the irradiation time (0-1200 s), the absorbance of the TiO_2 film (0.3 at 365 nm), and the energy of the photon, which has the wavelength of 365 nm.

## S3. Quantum Calculation of Optical Transitions of TDI, TDI Endoperoxide, and TDI Diepoxide.

To investigate the spectral blue-shift due to the cycloaddition of $^1O_2$ to TDI, optical transitions of the parent TDI, TDI endoperoxide, and TDI diepoxide have been determined using the time-dependent (TD) DFT approach (Gaussian 03, B3LYP/3-21G*).[24] The optimized structures, the peaks of the absorption wavelength, and its oscillator strength derived from the quantum calculation are shown in Figure S7. In this calculation, side chains, such as alkyl and phenyl groups (Figure S1), are substituted by hydrogen atoms for simplification. Figure S7D indicates the tendency of the spectral blue-shift due to the formation of the TDI diepoxide, although the absolute value of the wavelength (λ_{abs} = 654 nm for TDI in CHCl$_3$) is different. Thus, the quantum calculation strongly supports the formation of the TDI diepoxide, which would be deduced by observation of the spectral blue-shift of the TDI (from 670 nm to 610 nm).
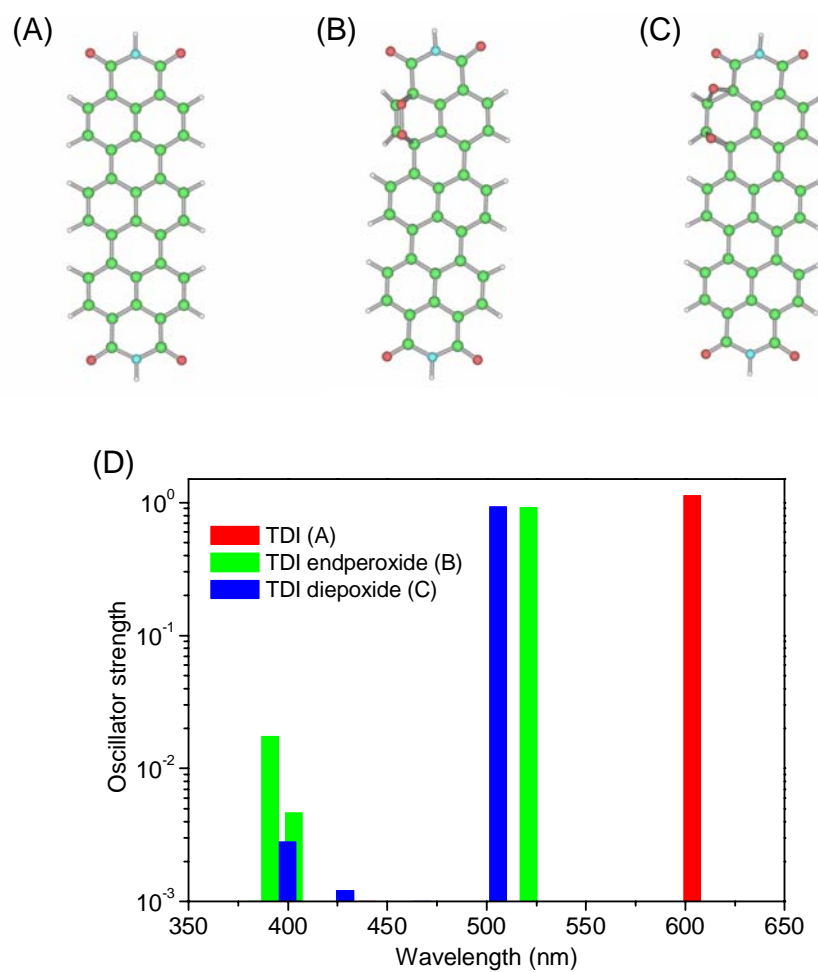
Figure S7. The optimized structure of TDI (A), TDI endoperoxide (B), and TDI diepoxide (C). The oscillator strength and the peaks of the absorption wavelength are shown (D).
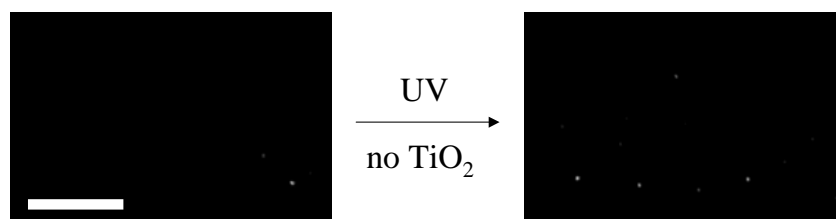
S4. Control Experiments.

All scale bars shown in the following images are 10 μm. When slide glass coated with TiO$_2$ film was used, several bright spots appeared after UV irradiation for 5 min.
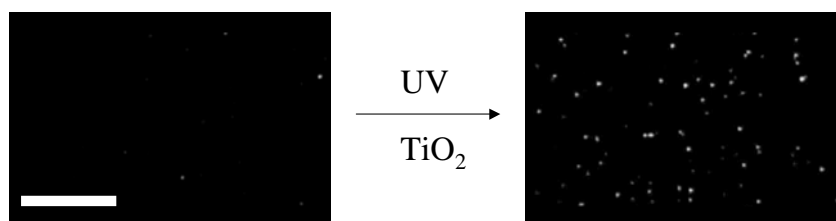
As a control, four experiments have been performed as follows:

1) in the absence of the TiO_2 film

Slide glass coated with no TiO_2 film was used.

2) in the absence of oxygen

To confirm that the formation of $^1O_2$ depends on the TiO_2 photocatalytic oxidation, the atmosphere in the sample was substituted from air to argon. Before the UV irradiation, argon gas was pumped into the sample for 10 min. To efficiently pump the argon gas into the sample, air holes are made on the TiO_2-coated slide glass (Figure S4).
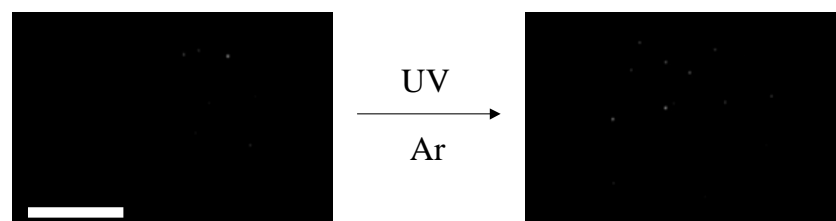

3) in the presence of $^1O_2$ quencher (DABCO)

To investigate whether or not the formation of the bright fluorescent spots (TDI diepoxide) is suppressed in the presence of the $^1O_2$ quencher (DABCO),[19] TDI, and DABCO are dissolved together in chloroform (3 nM, and 10 μM, respectively). The resulting TDI solution is spin-coated on the coverslip.
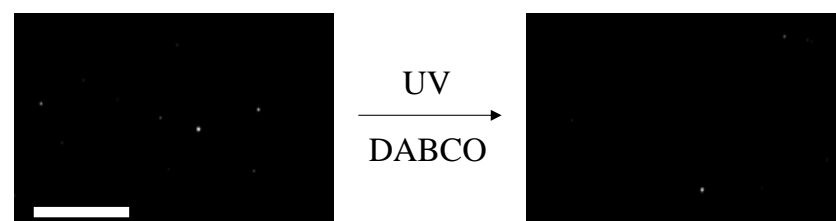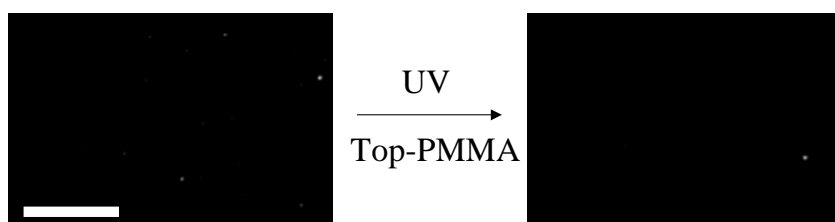
4) use of "top-coat" PMMA sample

To confirm the effect of the approach of airborne $^1O_2$, a PMMA film is fabricated on TDI molecules coated on a coverslip. The sample is shown in Figure S8.
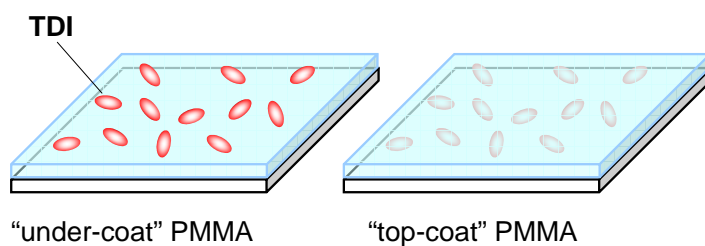
Figure S8. "under-coat" and "top-coat" PMMA.

In all the control experiments, the increase in the bright fluorescent spots (TDI diepoxide) was significantly suppressed, compared with that only using the TiO_2. The reasons are: the TiO_2 film and $^3O_2$ are required for the TiO_2 photocatalytic reactions. DABCO quenches $^1O_2$, which is required for the formation of the TDI diepoxide. The effect of the "top-coat" PMMA is interesting and important. The "top-coat" PMMA completely protects TDI from the approach of airborne $^1O_2$, as shown in Figure S9.
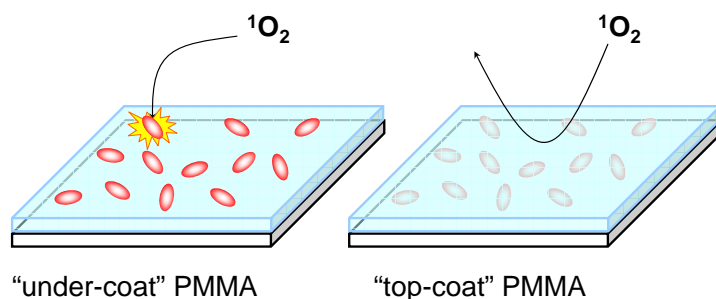
Figure S9. The protection of TDI from $^1O_2$ with "top-coat" PMMA.

References

(1) (a) Kautsky, H.; de Bruijn, H. *Naturwissenschaften* **1931**, *19*, 1043. (b) Kautsky, H.; Hirsch, A. *Chem. Ber.* **1931**, *64*, 2677-2683. (c) Kautsky, H.; de Bruijn, H.; Neuwirth, R.; Baumeister, W. *Chem. Ber.* **1933**, *66*, 1588-1600. (d) Kautsky, H. *Trans. Faraday Soc.* **1939**, *35*, 216-219.

(2) (a) Khan, A. U.; Kasha, M. *J. Chem. Phys.* **1963**, *39*, 2105-2106. (b) Khan, A. U.; Kasha, M. *Nature* **1964**, *204*, 241-243.

(3) Foote, C. S.; Wexler, S. *J. Am. Chem. Soc.* **1964**, *86*, 3879-3880.

(4) Corey, E. J.; Taylor, W. C. *J. Am. Chem. Soc.* **1964**, *86*, 3881-3882.

(5) Kearns, D. R. *Chem. Rev.* **1971**, *71*, 395-427, and references therein.

(6) Horiuchi, H.; Ishibashi, S.; Tobita, S.; Uchida, M.; Sato, M.; Toriba, K.; Otaguro, K.; Hiratsuka, H. *J. Phys. Chem. B* **2003**, *107*, 7739-7746.

(7) Snyder, J. W.; Zebger, I.; Gao, Z.; Poulsen, L.; Frederiksen, P. K.; Skovsen, E.; McIlroy, S. P.; Klinger, M.; Andersen, L. K.; Ogilby, P. R. *Acc. Chem. Res.* **2004**, *37*, 894-901, and references therein.

(8) For example, (a) Fujishima, A.; Rao, T. N.; Tryk, D. A. *J. Photochem. Photobiol. C: Photochem. Rev.* **2000**, *1*, 1-21. (b) Hoffmann, M. R.; Martin, S. T.; Choi, W.; Bahnemannt, D. W. *Chem. Rev.* **1995**, *95*, 69-96. (c) Mills, A.; Hunte, S. L. *J. Photochem. Photobiol. A* **1997**, *108*, 1-35.

(9) Nosaka, Y.; Daimon, T.; Nosaka, A. Y.; Murakami, Y. *Phys. Chem. Chem. Phys.* **2004**, *6*, 2917-2918.

(10) Hirakawa, K.; Hirano, T. *Chem. Lett.* **2006**, *35*, 832-833.

(11) Tatsuma, T.; Tachibana, S.; Miwa, T.; Tryk, D. A.; Fujishima, A. *J. Phys. Chem. B* **1999**, *103*, 8033-8035.

(12) (a) Tatsuma, T.; Tachibana, S.; Fujishima, A. *J. Phys. Chem. B* **2001**, *105*, 6987-6992. (b) Tatsuma, T.; Kubo, W.; Fujishima, A. *Langmuir* **2002**, *18*, 9632-9634. (c) Kubo, W.; Tatsuma, T.; Fujishima, A.; Kobayashi, H. *J. Phys. Chem. B* **2004**, *108*, 3005-3009.

(13) (a) Lee, M. C.; Choi, W.; *J. Phys. Chem. B* **2002**, *106*, 11818-11822. (b) Park, J. S. ; Choi, W. *Langmuir* **2004**, *20*, 11523-11527.

(14) (a) Haick, H.; Paz, Y. *J. Phys. Chem. B* **2001**, *105*, 3045-3051. (b) Haick, H.; Paz, Y. *Chem. Phys. Chem.* **2003**, *4*, 617-620.

(15) (a) Ishikawa, Y.; Matsumoto, Y.; Nishida, Y.; Taniguchi, S.; Watanabe, J. *J. Am. Chem. Soc.* **2003**, *125*, 6558-6562. (b) Lee, J. P.; Sung, M. M. *J. Am. Chem. Soc.* **2004**, *126*, 28-29.

(16) Murakami, Y.; Kenji, E.; Nosaka, A. Y.; Nosaka, Y. *J. Phys. Chem. B* **2006**, *110*, 16808-16811.

(17) Naito, K.; Tachikawa, T.; Fujitsuka, M.; Majima, T. *J. Phys. Chem. B* **2005**, *109*, 23138-23140.

(18) Holtrup, F. O.; Müller, G. R. J.; Quante, H.; De Feyter, S.; De Schryver, F. C.; Müllen, K. *Chem. -Eur. J.* **1997**, *3*, 219-225.

(19) Ogilby, P. R.; Iu, K.; Clough, R. L. *J. Am. Chem. Soc.* **1987**, *109*, 4746-4747.

(20) Linden, L. A.; Rabek, J. F.; Kaczmarek, H.; Kaminska, A.; Scoponi, M. *Coord. Chem. Rev*. **1993**, *125*, 195-218.

(21) Christ, T.; Kulzer, F.; Bordat, P.; Basché, T. *Angew. Chem. Int. Ed.* **2001**, *40*, 4192-4195.

(22) Jenny, T. A.; Turro, N. J. *Tetrahedron Lett.* **1982**, *23*, 2923-2926.

(23) Arbogast, J. W.; Darmanyan, A. P.; Foote, C. S.; Rubin, Y.; Diederich, F. N.; Alvarez, M. M.; Anz, S. J.; Whetten, R. L. *J. Phys. Chem.* **1991**, *95*, 11-12.

(24) Gaussian 03, Revision C.02, Frisch, M. J.; Trucks, G. W.; Schlegel, H. B.; Scuseria, G. E.; Robb, M. A.; Cheeseman, J. R.; Montgomery, Jr., J. A.; Vreven, T.; Kudin, K. N.; Burant, J. C.; Millam, J. M.; Iyengar, S. S.; Tomasi, J.; Barone, V.; Mennucci, B.; Cossi, M.; Scalmani, G.; Rega, N.; Petersson, G. A.; Nakatsuji, H.; Hada, M.; Ehara, M.; Toyota, K.; Fukuda, R.; Hasegawa, J.; Ishida, M.; Nakajima, T.; Honda, Y.; Kitao, O.; Nakai, H.; Klene, M.; Li, X.; Knox, J. E.; Hratchian, H. P.; Cross, J. B.; Bakken, V.; Adamo, C.; Jaramillo, J.; Gomperts, R.; Stratmann, R. E.; Yazyev, O.; Austin, A. J.; Cammi, R.; Pomelli, C.; Ochterski, J. W.; Ayala, P. Y.; Morokuma, K.; Voth, G. A.; Salvador, P.; Dannenberg, J. J.; Zakrzewski, V. G.; Dapprich, S.; Daniels, A. D.; Strain, M. C.; Farkas, O.; Malick, D. K.; Rabuck, A. D.; Raghavachari, K.; Foresman, J. B.; Ortiz, J. V.; Cui, Q.; Baboul, A. G.; Clifford, S.; Cioslowski, J.; Stefanov, B. B.; Liu, G.; Liashenko, A.; Piskorz, P.; Komaromi, I.; Martin, R. L.; Fox, D. J.; Keith, T.; Al-Laham, M. A.; Peng, C. Y.; Nanayakkara, A.; Challacombe, M.; Gill, P. M. W.; Johnson, B.; Chen, W.; Wong, M. W.; Gonzalez, C.; and Pople, J. A.; Gaussian, Inc., Wallingford CT, 2004.